Proceedings of the 16th International IEEE Annual Conference on Intelligent Transportation Systems (ITSC 2013), The Hague, The Netherlands, October 6-9, 2013

Immersion and Invariance Control for Reference Trajectory Tracking of Autonomous Vehicles

Gilles Tagne, Reine Talj and Ali Charara

Abstract— **This paper presents design and validation of a vehicle lateral controller for autonomous trajectory following based on Immersion and Invariance (*I&I*) principle. The aim is to minimize the lateral displacement of the autonomous vehicle with respect to a given reference trajectory. The control input is the steering angle and the output is the lateral displacement error. A first version of this controller based on *I&I* principle has been proposed previously by the authors in [1], but it suffers from a lack of robustness in some critical situations, near the nonlinear zones. In this paper, we propose a considerable improvement in the used model and the control synthesis. To validate the control strategy, the closed-loop system simulated on Matlab-Simulink has been compared to the experimental data acquired on the vehicle DYNA of Heudiasyc laboratory, a Peugeot 308, according to several real driving scenarios. The validation shows robustness and good performances of the proposed control approach, and puts in evidence the improvement with regard to the previous *I&I* control strategy proposed in [1].**

I. INTRODUCTION

Technological advances in recent years have favored the emergence of intelligent vehicles with the capacity to anticipate and compensate a failure (of driver, vehicle or infrastructure) or even to ensure an autonomous driving.

An autonomous navigation requires three main steps:

- The perception: it consists on detecting the dynamical environment of the vehicle including road, fix and mobile obstacles, etc... A vision system composed of sensors like cameras, lasers, radars and GPS is usually used to achieve this goal. It provides a dynamic map of the near environment of the autonomous vehicle.
- The path planning: it consists to generate and choose one trajectory (reference path) in the navigable space, according to several criteria.
- The vehicle control: it consists to handle the vehicle using actuators like brake, accelerator and steering wheel to follow the reference path.

This paper focus on the third main step that treats the vehicle control, more precisely, the lateral control of the intelligent vehicle. This is a very active research field that has been studied since the 1950s. Lateral control consists on automatically steering the vehicle to follow the reference trajectory. Given the high nonlinearity of the vehicle system on one hand, and the uncertainties and disturbances of such a system on the other hand, a very important issue to be considered in the control design is the robustness. The controller should be able to reject the disturbances caused by wind, coefficient of friction of the road and many other reasons, and able to deal with parameter uncertainties and variations.

For over 20 years, considerable research is conducted to provide lateral guidance of autonomous vehicles. Several control strategies have been developed in the literature. Simple Proportional (P) and Proportional-Integral (PI) controllers have been proposed in [2] and [3] respectively. Also a nested PID controller is presented in [4]. On the other hand, adaptive controllers have been developed for this application, as in [5]. Moreover, different other classical techniques have been applied: H_∞ control in [6], state feedback control in [7], Lyapunov stability based control in [8], artificial intelligence in [9], fuzzy logic in [10], linear quadratic optimal predictive control in [11], and many other techniques.

Robust control as the sliding mode technique has been applied to the lateral control in [12], [13], and [14]. This control strategy is well suited to driving conditions, given its robustness against uncertainties and its capacity to reject disturbances encountered in automotive applications. However, its main drawback is the chattering.

On the other hand, Model Predictive Control (MPC) appears to be well suited to the trajectory following [15], [16], [17]. It allows to consider the problem of trajectory tracking for nonlinear systems taking into account the constraints on the state variables and/or control inputs. However, the computation time increases considerably at high speed autonomous driving, what renders difficult the use of such method in real-time operation [11].

With such advances in this domain, the proposed controllers have been subject of several performance comparison as in [18], where a comparison is made between proportional, adaptive, H_∞ and fuzzy controllers. Different comparisons showed that the class of adaptive controllers represents a very promising technique for such uncertain and nonlinear application.

The Immersion and Invariance (*I&I*) principle is a relatively new method for designing nonlinear and adaptive controllers for (uncertain) nonlinear systems. The method relies upon the notions of system immersion and manifold invariance. The basic idea of the *I&I* approach is to achieve the control objective by immersing the plant dynamics into a (possibly lower-order) target system that captures the desired behavior [19]. This is achieved by finding a manifold in state-space that can be rendered invariant and attractive – with internal dynamics that reflect the desired closed-loop

The authors are working at Heudiasyc Laboratory, UMR CNRS 7253, Université de Technologie de Compiègne, BP 20529, 60205 Compiègne, France
gilles.tagne@hds.utc.fr, reine.talj@hds.utc.fr, ali.charara@hds.utc.fr

978-1-4799-2914-613/$31.00 ©2013 IEEE

dynamics– and by designing a control law that takes the state of the system towards the manifold.

In [1], we have developed a controller based on the *I&I* approach for autonomous lateral trajectory tracking. During validation with real data, we noticed that an offset appears in the lateral displacement error after an important solicitation of the vehicle near the nonlinear operating zone. This offset is due to the use of the yaw angle error in the control input, which is noisy variable and difficult to measure. To solve this problem, we have previously added a term of robustness to the control input to cancel the lateral error. In this paper, we propose a solution to the problem in the design of the *I&I* controller, where another state variables – reliable in measure or estimation [20]– are used to represent the vehicle dynamics. Moreover, this method allows to prove a very strong stability criterion of the closed–loop system with this *I&I* controller, for all controller gains chosen to be positive. Some interesting characteristics of the system are demonstrated and used to succeed to this result.

To design the controller, we consider that the vehicle is equipped with sensors and/or observers to measure sideslip angle, yaw rate, lateral error and its derivative. To validate the proposed approach, tests were made with real data acquired on the vehicle DYNA, on the tracks and circuits of CERAM[1]. The simulation results show the performance and robustness of the proposed approach.

This paper is organized as follows. Section II presents the dynamical models of the vehicle, used for control design and validation. In Section III, the *I&I* main principle is presented and the control strategy for lateral vehicle dynamics is developed. Section IV presents the simulation results and the performance validation of the proposed controller. Finally, we conclude in Section V, with some remarks and future work directions.

II. DYNAMIC MODELS OF VEHICLE

In this work, we use two vehicle models. The first one is the bicycle model used in Section III.B for the control design for its simplicity. The second is the 4-wheel vehicle model used to validate in simulation the proposed controller in closed-loop.

A. Bicycle model

To design the controller, a simple and widely used dynamic bicycle model [7] is considered. This model is used to represent the lateral vehicle behavior (lateral acceleration, yaw rate, sideslip angle) and assumes that the vehicle is symmetrical, and tire sideslip angles on the same axle are equal. The roll and pitch dynamics are neglected and angles are assumed to be small (steering, sideslip, yaw). With a linear tire force model we obtain a linear parameter varying (LPV) model, where the longitudinal velocity V_x is considered as a varying parameter. Dynamic equations in terms of slip angle and yaw rate of the bicycle model are given by:

$$\begin{cases} \dot{\beta} = -\frac{(C_f+C_r)}{mV_x}\beta - (1+\frac{L_fC_f-L_rC_r}{mV_x^2})\dot{\psi} + \frac{C_f}{mV_x}\delta \\ \ddot{\psi} = -\frac{L_fC_f-L_rC_r}{I_z}\beta - \frac{L_f^2C_f+L_r^2C_r}{I_zV_x}\dot{\psi} + \frac{L_fC_f}{I_z}\delta \end{cases} \quad (1)$$

where β and ψ represent respectively the sideslip angle and the yaw angle of the vehicle. Table I presents vehicle parameters and nomenclature.

TABLE I

VEHICLE PARAMETERS AND NOMENCLATURE (BICYCLE MODEL)

V_x	Longitudinal velocity	-	[m/s]
β	Sideslip angle	-	[rad]
$\dot{\psi}$	Yaw rate	-	[rad/s]
δ	Steering wheel angle	-	[rad]
m	Mass	1719	[kg]
I_z	Yaw moment of inertia	3300	[kgm^2]
L_f	Front axle-COG distance	1.195	[m]
L_r	Rear axle-COG distance	1.513	[m]
C_f	Cornering stiffness of the front tire	170550	[N/rad]
C_r	Cornering stiffness of the rear tire	137844	[N/rad]

B. 4-wheel model

To compare our simulation results with real data, we used a more representative model; namely, the 4-wheel model to represent the behavior of the vehicle and Dugoff's tire model for longitudinal and lateral forces [21].

III. *I&I* CONTROLLER DESIGN

After a brief presentation of the *I&I* principle and the controller developed above, we will present the design of a new controller.

A. I&I main principle

The developed controller is based on the following theorem, representing the main stabilization result of the Immersion and Invariance method.

Theorem 1: [19] Consider the system

$$\dot{x} = f(x) + g(x)u, \quad (2)$$

with $x \in \mathbb{R}^n$, $u \in \mathbb{R}^m$, and an equilibrium point $x^\star$ to be stabilized. Assume that there exist smooth mappings $\alpha : \mathbb{R}^p \to \mathbb{R}^p$, $\pi : \mathbb{R}^p \to \mathbb{R}^n$, $\phi : \mathbb{R}^n \to \mathbb{R}^{n-p}$, $c : \mathbb{R}^p \to \mathbb{R}^m$ and $v : \mathbb{R}^{nx(n-p)} \to \mathbb{R}^m$, with $p < n$, such that the following hold.

- (A1) The target system

$$\dot{\xi} = \alpha(\xi), \quad (3)$$

with $\xi \in \mathbb{R}^p$ has a globally asymptotically stable equilibrium at $\xi^\star \in \mathbb{R}^p$ and

$$x^\star = \pi(\xi^\star). \quad (4)$$

- (A2) For all $\xi \in \mathbb{R}^p$,

$$f(\pi(\xi)) + g(\pi(\xi))c(\pi(\xi))) = \frac{\partial \pi}{\partial \xi}\alpha(\xi). \quad (5)$$

- (A3) The set identity

$$\{x \in \mathbb{R}^n | \ \phi(x) = 0\} = \{x \in \mathbb{R}^n \mid x = \pi(\xi), \ \xi \in \mathbb{R}^p\} \quad (6)$$

[1]CERAM -"Centre d'Essais et de Recherche Automobile de Mortefontaine" is an automobile testing and research center located in France.

holds.

- (A4) All trajectories of the system

$$\dot{z} = \frac{\partial \phi}{\partial x}(f(x)+g(x)v(x,z)), \quad (7)$$
$$\dot{x} = f(x)+g(x)v(x,z), \quad (8)$$

are bounded and (7) has a uniformly globally asymptotically stable equilibrium at $z=0$.

Then $x^\star$ is a globally asymptotically stable equilibrium of the closed-loop system

$$\dot{x} = f(x)+g(x)v(x,\phi(x)). \quad (9)$$

□□□

Any trajectory $x(t)$ of the closed-loop system $\dot{x}=f(x)+g(x)v(x,\phi(x))$ is the image through the mapping $\pi(.)$ of a trajectory $\xi(t)$ of the target system. Note that the mapping $\pi:\xi\to x$ is an immersion, i.e., the rank of π is equal to the dimension of ξ. Then, the approach consists on applying a control law that renders the manifold $x=\pi(\xi)$ attractive and keeps the closed-loop trajectories bounded.

B. I&I Version 1 (I&I V1) controller

In [1], we have developed a controller based on the principle of Immersion & Invariance for autonomous lateral trajectory tracking. This controller is based on a bicycle model with the following state variables: the yaw angle error, the yaw rate error, the lateral displacement error and its derivative;

$$\chi = (\tilde{\psi}, \dot{\tilde{\psi}}, e, \dot{e})$$

with $\tilde{\psi}=\psi-\psi^\star$, the yaw angle error.

During validation we noticed that an offset appears in the lateral displacement error after an important solicitation of the vehicle near the nonlinear operating zone. This offset is due to the use of the yaw angle error in the control input, which is estimated by integrating the yaw rate error noisy in measurement. To solve this problem, we have previously added a term of robustness δ_{rob} to the control input, of the form:

$$\delta_{rob} = -\alpha \frac{|\dot{e}+\lambda e|}{|\dot{e}+\lambda e|+\varepsilon} \int sign(\dot{e}+\lambda e)\ , \quad (10)$$

to cancel the lateral error.

In this paper, we propose a solution to the problem in the design of the *I&I* controller, where another state variables –reliable in measure or estimation– are used to represent the vehicle dynamics. The proposed model reformulation avoids the use of the yaw angle error. Instead, the sideslip angle is used, this variable can be estimated as in [20].

C. I&I Version 2 (I&I V2) controller design

The lateral error dynamics at the center of gravity of the vehicle, with respect to a reference trajectory, is given by:

Sinnvoll?

$$\ddot{e} = a_y - a_{y_{ref}} \quad (11)$$

where a_y and $a_{y_{ref}}$ represent respectively the lateral acceleration of the vehicle, and the desired one on the reference trajectory. Assuming that the desired lateral acceleration of the vehicle can be written as $a_{y_{ref}} = V_x^2\rho$, where ρ is the curvature of the road and given that $a_y = V_x(\dot{\beta}+\dot{\psi})$, we have:

$$\ddot{e} = V_x(\dot{\beta}+\dot{\psi}) - {V_x}^2\rho \quad (12)$$

Replacing $\dot{\beta}$ by its expression in equation (1), we obtain:

$$\ddot{e} = -\frac{C_f+C_r}{m}\beta - \frac{L_fC_f-L_rC_r}{mV_x}\dot{\psi} - V_x^2\rho + \frac{C_f}{m}\delta \quad (13)$$

The new system state variables are the sideslip angle, the yaw rate, the lateral error and its derivative. The system has the following dynamics:

$$\dot{x} = Ax + B_1\delta + B_2\rho \quad (14)$$

where,

$$A = \begin{bmatrix} -\frac{(C_f+C_r)}{mV_x} & -1-\frac{(L_fC_f-L_rC_r)}{mV_x^2} & 0 & 0 \\ -\frac{(L_fC_f-L_rC_r)}{I_z} & -\frac{(L_f^2C_f+L_r^2C_r)}{I_zV_x} & 0 & 0 \\ -\frac{(C_f+C_r)}{m} & -\frac{(L_fC_f-L_rC_r)}{mV_x} & 0 & 0 \\ 0 & 0 & 1 & 0 \end{bmatrix}$$

$$B_1 = \begin{bmatrix} \frac{C_f}{mV_x} \\ \frac{L_fC_f}{I_z} \\ \frac{C_f}{m} \\ 0 \end{bmatrix}$$

$$B_2 = \begin{bmatrix} 0 \\ 0 \\ -V_x^2 \\ 0 \end{bmatrix}$$

The control input is the steering angle and the lateral displacement is the output. The aim of the lateral control is to cancel the lateral error displacement. Then, for a given curvature ρ and longitudinal velocity V_x, the desired behavior corresponds to $\dot{e}_1 = e_1 = 0$. Hence, it is easy to prove that the desired equilibrium point is [7]:

$$(\beta, \dot{\psi}, \dot{e}, e)^\top = (\beta^\star, \dot{\psi}^\star, 0, 0)^\top$$

with

$$\begin{aligned} \beta^\star &= V_x(L_r - \frac{L_fmV_x^2}{C_r(L_f+L_r)})\rho \\ \dot{\psi}^\star &= V_x\rho \end{aligned} \quad (15)$$

At the equilibrium point, the control input is:

$$\delta^\star = \frac{L_fC_f - L_rC_r}{L_fC_f}\beta^\star - \frac{L_f^2C_f + L_r^2C_r}{L_fC_fV_x}\dot{\psi}^\star \quad (16)$$

We define the new error variables:

$$\begin{cases} \tilde{\beta} = \beta - \beta^\star \\ \dot{\tilde{\psi}} = \dot{\psi} - \dot{\psi}^\star \\ \tilde{\delta} = \delta - \delta^\star \end{cases} \quad (17)$$

Hence, the error dynamics of the system (14) having the origin as equilibrium point $(\tilde{\beta}, \dot{\tilde{\psi}}, \dot{e}, e)^\top = (0,0,0,0)^\top$ become:

$$\dot{\tilde{x}} = A\tilde{x} + B_1\tilde{\delta} \quad (18)$$

where, A and B_1 have been defined above.

Now, consider the vehicle lateral dynamical model (18). As mentioned before, the main objective of the steering

controller is to cancel the lateral error displacement with respect to a given trajectory, then $e = \dot{e} = 0$ at the equilibrium. Hence, the target dynamical system (ξ_1, ξ_2) with $\xi_1 = \tilde{\beta}$ and $\xi_2 = \dot{\tilde{\psi}}$, has been chosen as the image of the system (18) when $e = \dot{e} = 0$. Notice that for $e = \dot{e} = 0$, we have also $\ddot{e} = 0$. The target dynamics can be expressed as follows,

$$\begin{bmatrix} \dot{\xi}_1 \\ \dot{\xi}_2 \end{bmatrix} = \begin{bmatrix} 0 & -1 \\ \frac{C_r(L_f+L_r)}{I_z} & -\frac{L_rC_r(L_f+L_r)}{I_zV_x} \end{bmatrix} \begin{bmatrix} \xi_1 \\ \xi_2 \end{bmatrix} \tag{19}$$

Proposition 1: The target model (19) has a globally asymptotically stable equilibrium at the origin $(0,0)$.

Proof: The dynamics of the state vector $\xi = [\xi_1, \xi_2]$ can be written in the form $\dot{\xi} = C\xi$, with

$$C = \begin{bmatrix} 0 & -1 \\ \frac{C_r(L_f+L_r)}{I_z} & -\frac{L_rC_r(L_f+L_r)}{I_zV_x} \end{bmatrix} \tag{20}$$

Then, after some simple calculations, we obtain:

$$\det(sI - C) = s^2 + \frac{L_rC_r(L_f+L_r)}{I_zV_x}s + \frac{C_r(L_f+L_r)}{I_z} \tag{21}$$

The matrix C verifies the Routh-Hurwitz stability criterion ($V_x > 0$), what yields to the desired result. ■

Proposition 2: Consider the system (18) having the equilibrium point at the origin. Moreover, the subsystem (19), which is the image of the system (18) for $e = \dot{e} = 0$, has a globally asymptotically stable equilibrium at the origin. Then, the system (18) is *I&I*-stabilisable with target dynamics (19).

Proof: We define now the off-the-manifold variable

$$z = \dot{e} + \lambda e, \quad \text{s.t.} \quad \lambda > 0 \tag{22}$$

We have to select a control input $\tilde{\delta}$ such that the trajectories of the closed-loop system are bounded and $z = \dot{e} + \lambda e$ converges to zero. Notice that, when $z \to 0$, e converges exponentially to zero with the rate of convergence λ. Then, $\dot{e}$ converges also to zero, yielding to the desired result.
To this end, let

$$\dot{z} = -Kz, \quad \text{with} \quad K > 0. \tag{23}$$

K represents the rate of exponential convergence of z to zero. Given the principle of the controller, it can be noticed that there are two manifolds, an outer manifold $\mathscr{M}_1$ reached when the off-the-manifold variable z converges exponentially to zero with the rate of convergence $K > 0$. Then, an inner manifold $\mathscr{M}_2$ can be reached from any point in $\mathscr{M}_1$ with the off-the-manifold variable e that converges exponentially to zero with the rate of convergence $\lambda > 0$.

Replacing $\dot{z}$ and z by their expressions in (23), and after some calculations, one can find that the corresponding control input has the following expression:

$$\tilde{\delta} = -\frac{m(K+\lambda)}{C_f}\dot{e} - \frac{mK\lambda}{C_f}e + \frac{C_f+C_r}{C_f}\tilde{\beta} + \frac{L_fC_f - L_rC_r}{C_fV_x}\dot{\tilde{\psi}} \tag{24}$$

The closed-loop system becomes:

$$\begin{bmatrix} \dot{\tilde{\beta}} \\ \ddot{\tilde{\psi}} \\ \ddot{e} \\ \dot{e} \end{bmatrix} = \left[\begin{array}{c|c} \mathscr{A}_{11} & \mathscr{A}_{12} \\ \hline \mathscr{A}_{21} & \mathscr{A}_{22} \end{array}\right] \begin{bmatrix} \tilde{\beta} \\ \dot{\tilde{\psi}} \\ \dot{e} \\ e \end{bmatrix} \tag{25}$$

with,

$$\mathscr{A}_{11} = \begin{bmatrix} 0 & -1 \\ \frac{C_r(L_f+L_r)}{I_z} & -\frac{L_rC_r(L_f+L_r)}{I_zV_x} \end{bmatrix} = C,$$
$$\mathscr{A}_{12} = \begin{bmatrix} \frac{-(K+\lambda)}{V_x} & \frac{-K\lambda}{V_x} \\ -\frac{L_fm(K+\lambda)}{I_z} & -\frac{L_fmK\lambda}{I_z} \end{bmatrix},$$
$$\mathscr{A}_{21} = \begin{bmatrix} 0 & 0 \\ 0 & 0 \end{bmatrix},$$
$$\mathscr{A}_{22} = \begin{bmatrix} -(K+\lambda) & -K\lambda \\ 1 & 0 \end{bmatrix}.$$

The closed-loop system can be interpreted as the interconnection of two subsystems: S_1 with the state variables ($\tilde{\beta}$ and $\dot{\tilde{\psi}}$), and S_2 (with the state variables $\dot{e}$ and e). Given that the interaction matrix $\mathscr{A}_{21}$ is identically zero, hence, the dynamics of the subsystem S_2 are independent of S_1, and can be written as follows:

$$\begin{bmatrix} \ddot{e} \\ \dot{e} \end{bmatrix} = \begin{bmatrix} -(K+\lambda) & -K\lambda \\ 1 & 0 \end{bmatrix} \begin{bmatrix} \dot{e} \\ e \end{bmatrix} \tag{26}$$

The subsystem S_2 combines and represents the interactions between the dynamics of both off-the-manifold variables z and e, which ensure convergence to the manifolds $\mathscr{M}_1$ and $\mathscr{M}_2$ respectively.

Proposition 3: The subsystem S_2 has a globally asymptotically stable equilibrium at the origin $(0,0)$.

Proof: The dynamics of the state vector $\zeta = [\dot{e}, e]$ can be written in the form : $\dot{\zeta} = \mathscr{A}_{22}\zeta$. The matrix $\mathscr{A}_{22}$ verifies the Routh-Hurwitz stability criterion, for all $\lambda > 0$ and $K > 0$, hence the attractivity of both manifolds is ensured. Then, the rates of convergence K and λ have to be chosen based on other practical considerations related to the system. ■

The subsystem S_1 depends on S_2 via the matrix $\mathscr{A}_{12}$. Defining $\tilde{u} = (K+\lambda)\dot{e} + K\lambda e$, the subsystem S_1 in closed-loop has the form:

$$\begin{bmatrix} \dot{\tilde{\beta}} \\ \ddot{\tilde{\psi}} \end{bmatrix} = \mathscr{A}_{11} \begin{bmatrix} \tilde{\beta} \\ \dot{\tilde{\psi}} \end{bmatrix} + \begin{bmatrix} -\frac{1}{V_x} \\ -\frac{L_fm}{I_z} \end{bmatrix} \tilde{u} \tag{27}$$

Finally it is clear that when S_2 converges to $(0,0)$, the input $\tilde{u}$ of the subsystem S_1 converges to zero. Then, the system S_1 converges to the target system, whose dynamics (19) is stable and converges to $(0,0)$. Indeed, we have proved previously that this target model has a globally asymptotically stable equilibrium at the origin $(0,0)$. So, the trajectories of the closed-loop system are bounded, yielding to the desired result. ■

Finally, the control input applied to the system (14) is:

$$\begin{aligned} \delta = \tilde{\delta} + \delta^\star = &-\frac{m(K+\lambda)}{C_f}\dot{e} - \frac{mK\lambda}{C_f}e + \frac{C_f+C_r}{C_f}\beta \\ &+ \frac{L_fC_f - L_rC_r}{C_fV_x}\dot{\psi} + \frac{mV_x^2}{C_f}\rho \end{aligned} \tag{28}$$

To apply our control law, the yaw rate, lateral error and its derivative are measured. The sideslip angle is estimated.

IV. SIMULATION RESULTS

The experimental data used here are acquired on the CERAM test circuits by the vehicle DYNA of Heudiasyc laboratory (Fig. 1). This vehicle is equipped with several sensors: an Inertial Measurement Unit (IMU) measuring accelerations (x, y, z) and the yaw rate, the CORREVIT for measuring the sideslip angle and longitudinal velocity, torque hubs for measuring tire-road efforts and vertical loads on each tire, four laser sensors to measure the height of the chassis, GPS and a CCD camera. Data provided via the CAN bus of the vehicle are also used, as the steering angle, and the rotational speed of the wheels.

Fig. 1. Experimental vehicle (DYNA)

To validate our control law, we perform several tests on the vehicle DYNA. The collected data are reference data that will be compared to those obtained by simulation of the closed–loop system with a complete 4-wheel vehicle model and the developed *I&I* controller. For the control law, we used the gains $\lambda = 8$ and $K = 1$, with the nominal vehicle parameters (see Table I). We compared the results of the controller that we developed previously [1], called *I&I* V1 with the one developed in this paper (*I&I* V2), to highlight the improvements. After that, we will perform tests of robustness with respect to parametric uncertainties and varriations of the new controller.

A. Test of the controller during normal driving

The first test (Figures 2, 3, 4 and 5) was carried out with the goal of verifying the robustness of the controller during normal driving. The lateral acceleration is less than $4m/s^2$. Longitudinal velocity is almost constant ($13.5m/s$).
Fig. 2 shows the longitudinal speed variations. Fig. 3 presents different curves: the reference path and the trajectory followed by the controlled vehicle ; the lateral deviation ; and the yaw angle error.

We observe that the *I&I* V1 controller and the *I&I* V2 can ensure the convergence to zero of the lateral error. After a large curvature, we note the presence of an offset in the measurement of the yaw rate. Hence, a bias appears in the yaw angle given that the latter is estimated by integrating the yaw rate. The *I&I* V1 controller depends on the yaw angle error, what renders the robustness of the controller weak, and subject for measures imprecisions. However, the

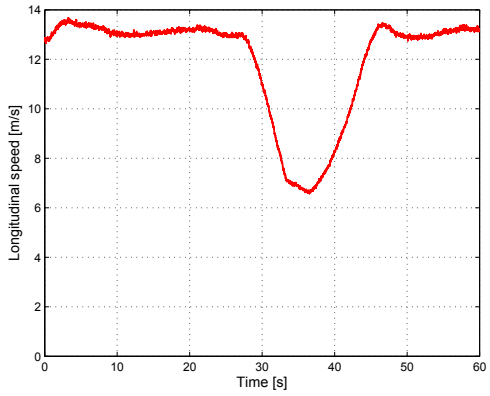

Fig. 2. Longitudinal speed

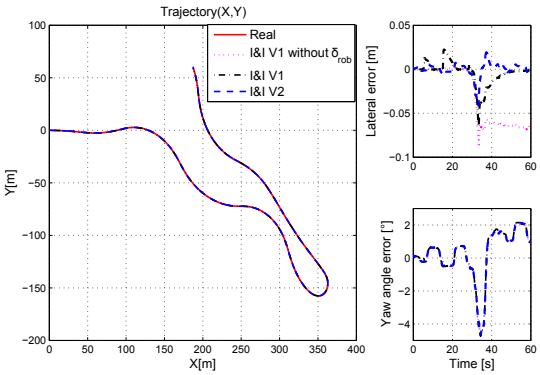

Fig. 3. Trajectories: Real (reference) and simulation (control laws)

I&I V2 controller is conceived in such a way to avoid the dependence on the fragile yaw angle error. Hence, this new controller allows to overcome the mentioned problem, it is able to track the reference path with small error under various conditions. The displacement from the guideline does not exceed $5cm$ in transient phase in this test conditions.
Fig. 4 presents dynamic variables of the vehicle: the steering angle, the yaw rate and the lateral acceleration. We compared the real data with data given by the simulated closed-loop system. Dynamic variables are very close to the measured ones. When the system is in the linear zone (e.g. for

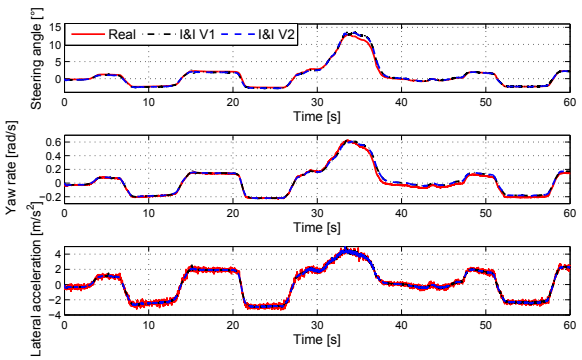

Fig. 4. Lateral acceleration, Steering angle and yaw rate

low steering angle), the controllers *I&I* V1 without robust term and *I&I* V2 have similar responses. In this case, the

robust term disturbs the system behavior (at low curvature variations), indeed it caused undesired peaks in the lateral error (see Fig. 3-b) and some oscillations in the control input (see Fig. 5). It therefore requires a delicate adjustment of the robustness term parameters, which is not obvious.

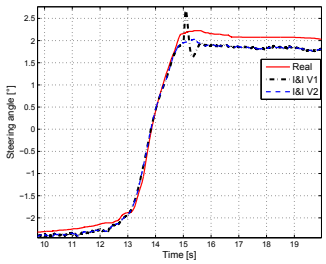

Fig. 5. Zoom of steering angle

In this scenario, although the assumption of small angles is not respected (the steering angle is greater than 12 degrees while turning), the new controller is able to follow the path with lower error than the previous. This first simulation shows the good performance and robustness of the controller. Note that in the previous controller, the addition of the robust term was necessary to follow the reference trajectory with low errors after a strong non-linearity. Moreover, an important improvement to be noticed is the smoothness of the control input (steering angle) with the new controller at the contrary of the previous one (Fig. 5).

B. Robustness of the controller during driving at high and varying speed

The Second test (Figures 6 and 7) was carried out with the goal of verifying the robustness of the controller during normal driving at high and varying speed. Longitudinal speed varies between $5m/s$ and $25m/s$. Note that the maximal lateral acceleration is $5m/s^2$. In this scenario we have some

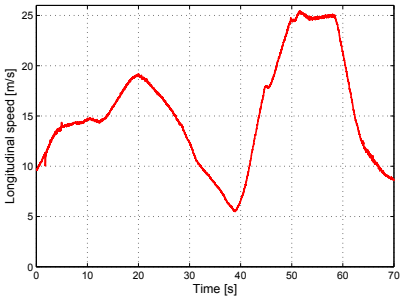

Fig. 6. Longitudinal speed

manoeuvres at low speed (large curvature) and at high speed. However, the lateral displacement of the closed–loop system remains smaller than $5cm$ in this test conditions, while the lateral error with the previous controller reaches $20cm$ (Fig. 7). The narrow peak of the *I&I* V1 shows that the *I&I* V2 is more robust to strong non-linearities caused by a large steering.

These two tests show the good performance and improvements of the new control strategy during normal driving at high and varying speed.

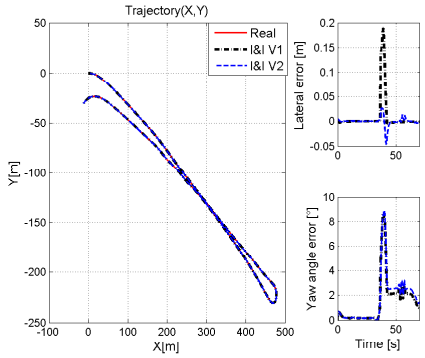

Fig. 7. Trajectories: Real (reference) and simulation (control laws)

C. Robustness of the new controller to vehicle parameters uncertainties

Several parameters of the vehicle can be uncertain, for example, the cornering stiffness, the mass, etc.

It is difficult to estimate accurately the cornering stiffness of the tire. Moreover, this parameter varies greatly depending on the type of road, the vertical load, camber, etc. It is therefore important to assess the robustness of the controller over cornering stiffness variations. Fig. 8 presents lateral errors for different cornering stiffness. Despite a $+/-30\%$ of variation in the value of cornering stiffness, the controller is able to follow the path with acceptable errors. In other words, the controller could be able to track the trajectory (giving acceptable errors) with a road coefficient of friction of 0.7. Indeed, the robustness of the controller against cornering stiffness variations, implicitly allows us to evaluate the robustness with respect to an unknown road coefficient of friction.

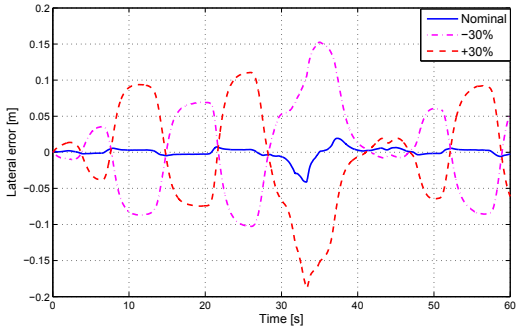

Fig. 8. Robustness against uncertainties of cornering stiffness

The mass of the vehicle may vary or be poorly estimated. It depends on the number of persons in the vehicle and the amount of fuel. We performed a last test concerning the robustness of the control law against the uncertainties on the vehicle mass (Fig. 9). For variations in the order of 10%, the error remain acceptable.

We note that large variations in the parameters degrade performance but stability is maintained. This clearly shows that we have a robust stability (do not depend on the value of the parameters of the system).

We also assess a test to evaluate the robustness of the controller to strong nonlinear dynamics. This test shows that

978-1-4799-2914-613/$31.00 ©2013 IEEE

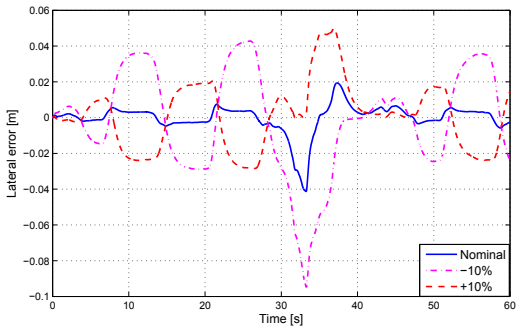

Fig. 9. Robustness against uncertainties of vehicle mass

the control law can ensure good behavior with high lateral accelarations up to $8m/s^2$. Finally, these results show the robustness of the controller.

V. CONCLUSIONS

In this paper, a lateral controller for autonomous vehicles has been proposed. This control strategy is based on the Immersion and Invariance theory to provide robust lateral tracking of a reference trajectory. An simulation validation has been done according to several scenarios representing different driving situations. The different tests performed highlight the robustness of the developed control law. Note that the robustness of the controlled system has been tested with respect to speed, curvature variations and parametric uncertainties /varriations (the cornering stiffness, the mass). The new controller has better performance than the previous one [1]. It achieves lower errors and a smooth steering. In addition, it is not necessary to add a term of robustness to ensure an exact path tracking even in high nonlinear situations at the limit of stability.

Stability of the system is assured with the proposed *I&I* controller for all its gains $\lambda > 0$ and $K > 0$. This is a very strong result that reveals some interesting characteristics of the system. More deep and promising characteristics of the system are under study now by the authors. Moreover, several parameters of the vehicle and its environment can be uncertain or varying, for example, the cornering stiffness, the mass, the road coefficient of friction etc. Then, in future work, we will study the stability and robustness of the proposed controller with respect to these parameters variations and uncertainties. We will do a thorough study of the system to define the performances (stability margins, robustness) for high speed driving. Also, we will do a comparative study with other control strategies to highlight the improvements of this strategy in terms of robust stability and robustness with respect to parametric uncertainties.

Moreover, our robotized vehicle arriving soon in the laboratory Heudiasyc, we will also test this control law on a semi-autonomous vehicle.

REFERENCES

[1] R. Talj, G. Tagne, and A. Charara, "Immersion and Invariance Control for Lateral Dynamics of Autonomous Vehicles , with Experimental Validation," in *European Control Conference*, (Zurich, Switzerland), pp. 968–973, 2013.

[2] A. Broggi, M. Bertozzi, and A. Fascioli, "The ARGO autonomous vehicle's vision and control systems," *Int. Journal of Intelligent Control and Systems*, vol. 3, no. 4, pp. 409–441, 1999.

[3] P. Zhao, J. Chen, T. Mei, and H. Liang, "Dynamic motion planning for autonomous vehicle in unknown environments," in *Int. IEEE Conference on Intelligent Vehicles Symposium (IV)*, June 2011.

[4] R. Marino, S. Scalzi, and M. Netto, "Nested PID steering control for lane keeping in autonomous vehicles," *Control Engineering Practice*, vol. 19, pp. 1459–1467, Dec. 2011.

[5] M. Netto, S. Chaib, and S. Mammar, "Lateral adaptive control for vehicle lane keeping," in *American Control Conference*, vol. 3, pp. 2693–2698, 2004.

[6] S. Hima, B. Lusseti, B. Vanholme, S. Glaser, and S. Mammar, "Trajectory Tracking for Highly Automated Passenger Vehicles," in *IFAC World Congress*, pp. 12958–12963, Aug. 2011.

[7] R. Rajamani, *Vehicle dynamics and control*. Springer, 2006.

[8] A. Benine-Neto, S. Scalzi, S. Mammar, and M. Netto, "Dynamic controller for lane keeping and obstacle avoidance assistance system," in *Int. IEEE Conference on Intelligent Transportation Systems*, pp. 1363–1368, Sept. 2010.

[9] E. Onieva, J. Naranjo, V. Milanés, J. Alonso, R. García, and J. Pérez, "Automatic lateral control for unmanned vehicles via genetic algorithms," *Applied Soft Computing*, vol. 11, pp. 1303–1309, Jan. 2011.

[10] J. Naranjo, C. Gonzalez, R. Garcia, and T. de Pedro, "Lane-Change Fuzzy Control in Autonomous Vehicles for the Overtaking Maneuver," *IEEE Transactions on Intelligent Transportation Systems*, vol. 9, pp. 438–450, Sept. 2008.

[11] D. Kim, J. Kang, and K. Yi, "Control strategy for high-speed autonomous driving in structured road," in *Int. IEEE Conference on Intelligent Transportation Systems (ITSC)*, Oct. 2011.

[12] J. Ackermann, J. Guldner, W. Sienel, R. Steinhauser, and V. Utkin, "Linear and nonlinear controller design for robust automatic steering," *IEEE Transactions on Control Systems Technology*, vol. 3, pp. 132–143, Mar. 1995.

[13] P. Hingwe and M. Tomizuka, "Experimental evaluation of a chatter free sliding mode control for lateral control in AHS," in *American Control Conference*, vol. 5, 1997.

[14] G. Tagne, R. Talj, and A. Charara, "Higher-Order Sliding Mode Control for Lateral Dynamics of Autonomous Vehicles , with Experimental Validation," in *Int. IEEE Conference on Intelligent Vehicles Symposium (IV)*, (Gold Coast, Australia), pp. 678–683, 2013.

[15] J. Levinson, J. Askeland, J. Becker, J. Dolson, D. Held, S. Kammel, J. Z. Kolter, D. Langer, O. Pink, V. Pratt, M. Sokolsky, G. Stanek, D. Stavens, A. Teichman, M. Werling, S. Thrun, and A. Hardware, "Towards Fully Autonomous Driving : Systems and Algorithms," in *Intelligent Vehicles Symposium (IV)*, 2011.

[16] P. Falcone, F. Borrelli, H. E. Tseng, J. Asgari, and D. Hrovat, "Linear time varying model predictive control and its application to active steering systems: Stability analysis and experimental validation," *Int. J. Robust Nonlinear Control*, vol. 18, pp. 862–875, 2008.

[17] T. Besselmann and M. Morari, "Autonomous Vehicle Steering Using Explicit LPV-MPC," in *European Control Conference*, (Budapest, Hungary), pp. 2628–2633, 2009.

[18] S. Chaib, M. Netto, and S. Mammar, "H inf, adaptive, PID and fuzzy control: a comparison of controllers for vehicle lane keeping," in *Int. IEEE Intelligent Vehicles Symposium (IV)*, 2004.

[19] A. Astolfi, D. Karagiannis, and R. Ortega, *Nonlinear and Adaptive Control with Applications*. Springer, 2008.

[20] M. Doumiati, A. Charara, A. Victorino, and D. Lechner, *Vehicle Dynamics Estimation using Kalman Filtering: Experimental Validation*. Wiley-ISTE, 2012.

[21] H. Dugoff, P. Fancher, and L. Segel, "An Analysis of Tire Traction Properties and Their Influence on Vehicle Dynamic Performance," *SAE*, 1970.